Difference Image Analysis of the OGLE-II Bulge Data. III. Catalog of 200,000 Candidate Variable Stars.*

P. R. Woźniak[1,2], A. Udalski[3], M. Szymański[3], M. Kubiak[3], G. Pietrzyński[3,4], I. Soszyński[3], K. Żebruń[3]

[1] *Princeton University Observatory, Princeton, NJ 08544, USA*

[2] *Los Alamos National Laboratory, MS-D436, Los Alamos, NM 87545, USA*

e-mail: wozniak@lanl.gov

[3] *Warsaw University Observatory, Al. Ujazdowskie 4, 00-478 Warszawa, Poland*

e-mail: (udalski,msz,mk,pietrzyn,soszynsk,zebrun)@astrouw.edu.pl

[4] *Universidad de Concepción, Departamento de Fisica, Casilla, 160-C, Concepción, Chile*

e-mail: pietrzyn@hubble.cfm.udec.cl

ABSTRACT

We present the first edition of a catalog of variable stars from OGLE-II Galactic Bulge data covering 3 years: 1997–1999. Typically 200–300 I band data points are available in 49 fields between −11 and 11 degrees in galactic longitude, totaling roughly 11 square degrees in sky coverage. Photometry was obtained using the Difference Image Analysis (DIA) software and tied to the OGLE data base with the DoPhot package. The present version of the catalog comprises 221,801 light curves. In this preliminary work the level of contamination by spurious detections is still about 10%. Parts of the catalog have only crude calibration, insufficient for distance determinations. The next, fully calibrated, edition will include the data collected in year 2000. The data is accessible via FTP. Due to the data volume we, also distribute DAT tapes upon request.

Based on observations obtained with the 1.3-m Warsaw telescope at Las Campanas Observatory of the Carnegie Institution of Washington

1. Introduction

The main goal of the Optical Gravitational Lensing Experiment (OGLE, Udalski, Kubiak & Szymański 1997) is to search for microlensing events. Observationally, these events are basically a rare type of an optical variable, therefore it came as no surprise that after several years microlensing experiments have an exceptional record of variability in terms of the number of objects and epochs. To maximize event rates, microlensing searches focus on monitoring of very crowded, and scientifically attractive, stellar fields; the Galactic Bulge region and Magellanic Clouds. Some observations are conducted in denser portions of the Galactic disk.

It is a common situation nowadays that the ability to generate data far exceeds the ability to process it, and even more so, to comprehend it. The list of projects which aim at monitoring significant parts of the sky for variability includes more than 30 names (*http://www.astro.princeton.edu/faculty/bp.html*), yet only a small fraction of those can process the data efficiently enough to make the measurements publicly available soon after the data is taken (e.g. Brunner et al. 2001). The issue of exporting the data in a convenient form compounds the problem. The National Virtual Observatory (NVO) project has very ambitious plans to provide the tools and some standards (perhaps de facto standards) for processing the large amounts of information and web data publication (Szalay 2001). Large catalogs have added complexity (project description *http://www.us-vo.org/*). By the time some sort of processing is complete, new information emerges in the process, frequently information which should be incorporated into the catalog. It seems that the only static layer is the raw data itself, typically CCD images, however the photometric output from number crunchers should also be reasonably slow to change with the new developments.

A regular practice in OGLE is to release the data in the public domain as soon as possible. The most significant contributions are: BVI maps of dense stellar regions (Udalski et al. 1998b, 2000a), Cepheids in Magellanic Clouds (Udalski et al. 1999a, 1999b), eclipsing variables in the SMC (Udalski et al. 1998a), catalogs of microlensing events (Udalski et al. 2000b, Woźniak et al. 2001). Examples from other microlensing teams include samples of MACHO microlensing events (Alcock et al. 1997a, 1997c) and selected variable star work from MACHO (1997b) and EROS (Afonso et al. 1999). In real time detection of microlensing events the main benefit comes from the follow-up work (e.g. Sackett 2000), in practice only possible with immediate publication on the WWW. Therefore, all major microlensing teams (OGLE, EROS, MACHO and MOA) have, or had, active alert systems.

A recent contribution to the publicly available data on variable stars is a WWW interface to the MACHO database (Allsman & Axelrod 2001), which started with somewhat limited features, but has plans for expansion. Similar ideas of making evolving catalogs have been discussed within OGLE for some time now and are motivated by the challenges of data processing/accessibility. The main objective here is not to make a potential broad user wait for a long time until the team makes the final refined product. There is a lot of potential use from the data at all levels of processing. OGLE has just released an online catalog of ~70,000 candidate variables in the LMC and SMC (Żebrun, Soszyński et al. 2001). With this paper we release an initial catalog of 221,801 candidate variables in the Galactic Bulge from Difference Image Analysis of OGLE-II data from seasons 1997-1999. Parts of the current edition are still not fully calibrated and should not be used in distance estimates (Section 3).

We restate the basic information about the data in Section 2 and in Section 3 we briefly summarize the process of finding variability. Section 4 gives the details of how the catalog is structured, followed by final remarks and future plans in Section 5.

2. Data

All OGLE-II frames were collected with the 1.3 m Warsaw Telescope at the Las Campanas Observatory, Chile. The observatory is operated by the Carnegie Institution of Washington. The "first generation" OGLE camera uses a SITe 2048×2049 CCD detector with 24μm pixels resulting in $0.417''$ pixel^{-1} scale. Images of the Galactic bulge are taken in drift-scan mode at "medium" readout speed with a gain of 7.1 e^-/ADU and readout noise of 6.3 e^-. The saturation level is about 55,000 ADU. For details of the instrumental setup, we refer the reader to Udalski, Kubiak & Szymański (1997).

The majority of frames were taken in the I photometric band. The effective exposure time is 87 seconds. During observing seasons of 1997–1999 the OGLE experiment typically collected between 200 and 300 I-band frames for each of the 49 bulge fields BUL_SC1–49. OGLE-II images are 2k×8k strips, corresponding to $14' \times 57'$ in the sky, therefore the total area of the bulge covered is about 11 square degrees. The number of frames in V and B bands is small and we do not analyze them with the DIA method. The median seeing is $1.3''$ for our data set. In Table 1 we provide equatorial and galactic coordinates of the field centers, the total number of analyzed frames and the number of candidate variables detected. Figure 1 schematically shows locations of the OGLE-II bulge fields with respect to the Galactic bar. Fields BUL_SC45 and BUL_SC46 were observed much less frequently, mostly with the purpose of maintaining phases of variable stars discovered by OGLE-I. Observations of fields BUL_SC47–49 started in 1998; the season of 1997 is not available for them.

3. Extracting variability from OGLE-II bulge frames using DIA

The DIA data pipeline we used is based on the image subtraction algorithm developed by Alard & Lupton (1998) and Alard (2000), and was written by Woźniak (2000). Processing of a large 2k×8k pixel frame is performed after dividing it into 512×128 pixel subframes, with 14 pixel margin to ensure smooth transitions between coordinate transformations and fits to spatially variable PSF for individual pieces. Small subframe size allows us to use polynomial fits for drift-scan images, in which PSF shape and local coordinate system vary on scales of 100–200 pixels. The reference image, subtracted from all images of any given field, is a stack of 20 best images in the sequence.

We adopted kernel expansion used by Woźniak (2000), generally applicable to all OGLE-II data. The kernel model, represented by a 15×15 pixel raster, consists of 3 Gaussians with sigmas 0.78, 1.35, and 2.34 pixels, multiplied by polynomials of orders 4, 3, and 2 respectively. The pipeline delivers a list of candidate variable objects and their difference light curves. The initial filtering is very weak, with only a minimum of assumptions made about the variability type. Candidate variables are flagged as "transient" or "continuous" variables depending on whether variability is confined to episodes in an otherwise quiet object, or spread throughout the observed time interval. The total number of candidate variables in all 49 fields was slightly over 220,000, including 150,000 "continuous" and 66,000 "transient" cases. Only 4600 objects passed both filters, confirming sensible definitions of classes. The number of detected variable objects in a given field depends on the number density of stars, extinction, and number of available measurements. This ranged from about 800 to over 9000 per field. The photometry files distributed with this publication do not contain some of the auxiliary information provided by the pipeline. In binary format they amount to slightly over 1.3 GB. Reference images take additional 1.6 GB of storage. We compress the data when possible.

The error distribution in measurements from our DIA pipeline is nearly Gaussian with the average scatter only 17% above the Poisson limit for faint stars near I=17–19 mag, gradually increasing for brighter stars, and reaching 2.5 times photon noise at $I \sim 11$ mag (about 0.5% of the total flux). Error bars adopted in this paper are photon noise estimates renormalized using the curve of Woźniak (2000). As the method effectively monitors all pixels, variable objects may be discovered even where no object is detected in the reference image. In regular searches monitoring is conducted only for objects detected in a single good quality image, a template. This issue is related to centroid finding. Currently in our DIA pipeline centroids are calculated based on the variable signal in a number of frames. As a result the centroid will be poorly known for an object with low S/N variability, even if it is very bright on the reference image. Ideally one would use both pieces of information. It is usually obvious how to determine the centroid in the presence of blending when confronted with one particular object of interest, but an optimal algorithm for extracting all variability in the field using DIA is yet to be developed.

Difference fluxes were converted to magnitudes using reference flux values obtained from DoPhot photometry on reference frames. The process of matching units was identical to that in Woźniak (2000). DIA observations were tied to the OGLE database of regular PSF photometry. Most fields were calibrated to 0.05 mag accuracy, however at the time of this analysis for 10 fields (BUL_SC: 7, 9, 20, 25, 28, 32, 43, 47, 48 and 49) only rough calibration was available and the zero point differences may reach ± 0.25 mag. The catalog will be re-calibrated after merging with the data for the 2000 observing season.

The conversion is given by the formula

$$m_I = m_0 - 2.5 \log(f + f_{\rm ref}),$$

where f is the difference flux of a particular observation, $f_{\rm ref}$ is the reference flux, m_0 is the magnitude zero point for a given subframe of the reference image, and m_I is the converted I-band magnitude. All quantities in the formula are available in the catalog and light curve files (Section 4). Due to noise, occasionally one runs into a problem of negative fluxes in DIA. For those measurements the difference flux may still be perfectly valid, the magnitude will have an error code and the appropriate flag will be set (Section 4 and Appendices).

Julian dates of individual observations also bear some discussion. In drift-scan observing the time of mid exposure depends on the position of the object. In the case of the Galactic Bulge data of OGLE-II, the correction which should be added to the starting time of the scan is given by:

$$dt = (Y + 1024) \times 0.0423816/86400 \qquad HJD < 2451040$$
$$dt = (Y + 1024) \times 0.0484627/86400 \qquad HJD \geq 2451040,$$

where Y is the pixel position in the reference image along the direction of the scan, in the range 0–8192 in OGLE-II, resulting in differences reaching several minutes. The time stamps of observations in the catalog have been corrected for this effect (Section 4).

4. FTP catalog

The catalog of candidate bulge variables presented in this paper is available via FTP from *ftp://bulge.princeton.edu/ogle/ogle2/bulge_dia_variables*. The data is naturally divided into 49 parts for fields BUL_SC1 – BUL_SC49. Reference images for each field (2k × 8k FITS frames) are stored in the subdirectory `reference_frames`. Information is available in two formats: plain text (subdirectory `plain_text`) and binary FITS tables (subdirectory `fits_tables`). FITS format is an astronomical standard and the ease of its use with programs like IDL is remarkable. There are two types of files for each field: the catalog of candidate variables, and the database of light curves. The catalog contains a single entry per object with the overall parameters of the light curve and identifying information, like coordinates. Below is a sample record with the explanation of fields:

3764 207.14 6721.60 271.272315 −28.578460 18:05:05.35 −28:34:42.5

17.407 0.783 359.5 23.38 0.13 1 152 0 181 181 1

1. [ ] — number of candidate variable as returned by the pipeline
2. [`X_TPL`] — x template coordinate (0.0 is the middle of the bottom left pixel)
3. [`Y_TPL`] — y template coordinate (0.0 is the middle of the bottom left pixel)
4. [`RA`] — RA in decimal degrees
5. [`DEC`] — DEC in decimal degrees
6. [`RA_STR`] — RA in sexagesimal hours
7. [`DEC_STR`] — DEC in sexagesimal degrees
8. [`MEAN_MAG`] — mean of all magnitude values which could be determined
9. [`MAG_SCAT`] — scatter of all magnitudes used in mean calculation
10. [`REF_FLUX`] — reference flux
11. [`MAG_0`] — magnitude zero point
12. [`ID_RAD`] — distance between the centroid of the variable and the nearest DoPhot star in the reference image in pixels (for the calculation of the reference flux and conversion to magnitudes)

13. [VTYPE] — type of variable coded in bits of a 2 byte integer: 1st bit – “transient”, 2nd bit – “continuous”. Therefore the value of the integer will be 1 for “transient”, 2 for “continuous variable ”, and 3 for both (see Section 3 for details).

14. [N_FRAMES] — number of frames used in centroid determination

15. [N_BAD] — number of bad pixels in the fitting radius on the reference image

16. [NGOOD] — number of “good” flux measurements. A “good” point is the one for which non of the several types of problems monitored by the pipeline occurred (flags 1–10 in Appendix B are set to 0).

17. [NMAG] — number of magnitude values which could be determined (the ones which are not determined come from non-positive fluxes)

18. [FLAG] — flags, see the explanation below

Several kinds of problematic situations are reported as flags in the last column of the catalog file. Flags are explained in Appendix A.

Capitalized names after the column number are names of columns in binary FITS tables (bul_sc*_cat.fts). An empty bracket means that this column is omitted in the FITS table, but it is present in the text file. In text version of these files (bul_sc*_cat.dat) columns have no names and are identified by their order. The database of light curves includes all measurements for all detected objects. Light curves in plain text format are stored one per file and grouped by the field. For example, subdirectory BUL_SC1 in plain_text contains 4597 bul_sc1_*.dat.gz files, compressed to save space and transfer time. The columns in light curve files are as follows:

1. [OBS_TIME] — Heliocentric Julian Day of the observation, offset by 2450000.0

2. [DIFF_FLUX] — difference flux (-99.00 for error code)

3. [FLUX_ERR] — difference flux error (-99.00 for error code)

4. [MAG] — I band magnitude (-1.0 for error code)

5. [MAG_ERR] — I band magnitude error (-1.0 for error code)

6. [FLAG] — flags, explained below

The flags are explained in Appendix B. They provide a lot of information on whether the measurement is valid or not and common problems which may have affected its reliability. To stay on the conservative side, only measurements with no flags should be used (integer value 0). In `plain_text` subdirectory there are also 49 `bul_sc*_db.tar` files with all light curve files for a given field grouped together for convenient transfers.

In binary FITS format all light curves for each field are stored in a single table. The first extension contains the names of the frames and starting times of the drift-scan exposures in Heliocentric Julian Days shifted by 2450000.0. These time stamps are identical for all objects in a single image. However, the effective time of mid exposure varies depending on the position of the object along the scan. The corrected times of observations are provided for each star separately in the second FITS extension with the actual photometry (Section 3). All measurements for all stars are stored in the same columns and identified by their index within the column. The number of observations per star is fixed and given by the length of the time vector from the first extension. Ordering is such that the number of the individual observation within a single light curve is ascending fastest along the column of the binary table. If, for example, the number of dates in the first extension of `bul_sc1_db.fts` is 197, the first 197 rows of the second FITS extension correspond to the first light curve, the next 197 rows are the second light curve and so on. The total number of rows is 197×4597, where 4597 is the number of candidate variables in BUL_SC1 field, the same as the number of rows in catalog files `bul_sc1_cat.dat` and `bul_sc1_cat.fts`. This information, along with several other useful numbers, is stored in headers.

In Appendix C we include the explanation and values of the pipeline parameters which were important for detection of variables.

5. Discussion and future work

As mentioned before, the current edition of the catalog basically includes entire output of the DIA pipeline as described by Woźniak (2000), supplemented with determinations of the reference flux to put the light curves on the magnitude scale. Some optimization has been performed to keep the contamination by artifacts low without rejecting too many real variable objects, but it must be clearly stated that about 10% of the light curves in the present release are not real objects and result from various problems, undetected at the pipeline level. We are extending the work of Mizerski & Bejger (2001) from the first BUL_SC1 field to all fields in the effort to flag several common types of artifacts and clean the sample of spurious objects.

Classifying a real variable star versus a spurious one is the first step in the interpretation of this data. Ultimately we envision increasingly refined information added to the catalog to facilitate applications. This should include the full classification of the detected variables, cross identification with objects found by 2MASS and in X-ray catalogs, periods for periodic sources etc. The work on automated classification of periodic variables is in progress. In addition to examining 2-D projections of a multidimensional parameter space and trying to code a human made algorithm (see Mizerski & Bejger 2001 and Woźniak et al. 2001 for such work on this data), we are experimenting with data mining techniques. Even with the current volume of data in OGLE-II we believe it is enabling to make the transition from "telling the computer how to do it" to "telling the computer what to do" and leaving the rest to the algorithm. A number of standard machine learning tools are available, which take small preclassified subsets of light curves and can "learn" to classify the rest of the data.

Żebrun, Soszyński et al. (2001) provided a convenient web interface to access the data on variables in the LMC and SMC. It is our intention to build a similar tool with the addition of positional searches. Although the volume of the data which can be accessed by browsing web pages is limited in practice, the search by coordinates is a powerful tool for numerous applications. Transfer by FTP and distribution of DAT tapes are currently primary modes of accessing major parts of this catalog. For your copy of a DAT tape, please contact Prof. Bohdan Paczyński (email: bp@astro.princeton.edu, mail: Princeton University Observatory, Princeton, NJ, 08544). To access this archive online use the OGLE web site *http://bulge.princeton.edu/~ogle/ogle2/bulge_dia_variables* .

We thank Prof. Paczyński for support and encouragement in this project. This work was supported by the NSF grant AST-9820314 to B. Paczyński, and Polish KBN grant 2P03D01418 to M. Kubiak. Additional support for P. Woźniak was provided under the DOE contract W-7405-ENG-36.

Table 1. OGLE-II bulge fields.

Field	α_{2000} h m s	δ_{2000} $\circ$ $'$ $''$	l $\circ$	b $\circ$	N_{obs}	N_{var}
BUL_SC1	18:02:32.5	−29:57:41	1.08	−3.62	197	4597
BUL_SC2	18:04:28.6	−28:52:35	2.23	−3.46	192	5279
BUL_SC3	17:53:34.4	−29:57:56	0.11	−1.93	309	8493
BUL_SC4	17:54:35.7	−29:43:41	0.43	−2.01	324	9096
BUL_SC5	17:50:21.7	−29:56:49	−0.23	−1.33	307	7257
BUL_SC6	18:08:03.7	−32:07:48	−0.25	−5.70	228	3211
BUL_SC7	18:09:05.5	−32:07:10	−0.14	−5.91	219	1618
BUL_SC8	18:23:06.2	−21:47:53	10.48	−3.78	211	2331
BUL_SC9	18:24:00.0	−21:47:10	10.59	−3.98	212	1847
BUL_SC10	18:20:06.6	−22:23:03	9.64	−3.44	220	2499
BUL_SC11	18:21:06.5	−22:23:05	9.74	−3.64	215	2256
BUL_SC12	18:16:06.3	−23:57:54	7.80	−3.37	209	3476
BUL_SC13	18:17:02.6	−23:57:44	7.91	−3.58	208	3084
BUL_SC14	17:47:02.7	−23:07:30	5.23	2.81	209	4051
BUL_SC15	17:48:06.9	−23:06:09	5.38	2.63	204	3853
BUL_SC16	18:10:06.7	−26:18:05	5.10	−3.29	202	4802
BUL_SC17	18:11:03.6	−26:12:35	5.28	−3.45	200	4690
BUL_SC18	18:07:03.5	−27:12:48	3.97	−3.14	203	5805
BUL_SC19	18:08:02.4	−27:12:45	4.08	−3.35	195	5255
BUL_SC20	17:59:16.0	−28:52:10	1.68	−2.47	235	5910
BUL_SC21	18:00:22.3	−28:51:45	1.80	−2.66	238	7449
BUL_SC22	17:56:47.6	−30:47:46	−0.26	−2.95	275	5589
BUL_SC23	17:57:54.5	−31:12:36	−0.50	−3.36	255	4815
BUL_SC24	17:53:17.9	−32:52:45	−2.44	−3.36	250	4304
BUL_SC25	17:54:21.0	−32:52:10	−2.32	−3.56	243	3046
BUL_SC26	17:47:15.5	−34:59:31	−4.90	−3.37	241	4713
BUL_SC27	17:48:23.6	−35:09:32	−4.92	−3.65	220	3691
BUL_SC28	17:47:00.0	−37:07:10	−6.76	−4.42	217	1472
BUL_SC29	17:48:10.8	−37:07:21	−6.64	−4.62	211	2398
BUL_SC30	18:01:25.0	−28:49:55	1.94	−2.84	233	6893

Table 1—Continued

Field	α_{2000} h m s	δ_{2000} ° ′ ″	l °	b °	$N_{\rm obs}$	$N_{\rm var}$
BUL_SC31	18:02:22.6	−28:37:21	2.23	−2.94	236	4789
BUL_SC32	18:03:24.0	−28:37:10	2.34	−3.14	231	5007
BUL_SC33	18:05:30.9	−28:52:50	2.35	−3.66	187	4590
BUL_SC34	17:58:18.5	−29:07:50	1.35	−2.40	239	7953
BUL_SC35	18:04:28.6	−27:56:56	3.05	−3.00	177	5169
BUL_SC36	18:05:31.2	−27:56:44	3.16	−3.20	209	8805
BUL_SC37	17:52:32.2	−29:57:44	0.00	−1.74	305	8367
BUL_SC38	18:01:28.0	−29:57:01	0.97	−3.42	191	5072
BUL_SC39	17:55:39.1	−29:44:52	0.53	−2.21	318	7338
BUL_SC40	17:51:06.1	−33:15:11	−2.99	−3.14	205	4079
BUL_SC41	17:52:07.2	−33:07:41	−2.78	−3.27	208	4035
BUL_SC42	18:09:05.0	−26:51:53	4.48	−3.38	204	4360
BUL_SC43	17:35:10.0	−27:10:10	0.37	2.95	251	3351
BUL_SC44	17:49:22.4	−30:02:45	−0.43	−1.19	258	7836
BUL_SC45	18:03:33.0	−30:05:00	0.98	−3.94	88	2262
BUL_SC46	18:04:36.0	−30:05:00	1.09	−4.14	84	2057
BUL_SC47	17:27:00.0	−39:46:00	−11.19	−2.60	151	1152
BUL_SC48	17:28:10.0	−39:46:00	−11.07	−2.78	145	973
BUL_SC49	17:29:20.0	−40:16:00	−11.36	−3.25	142	826

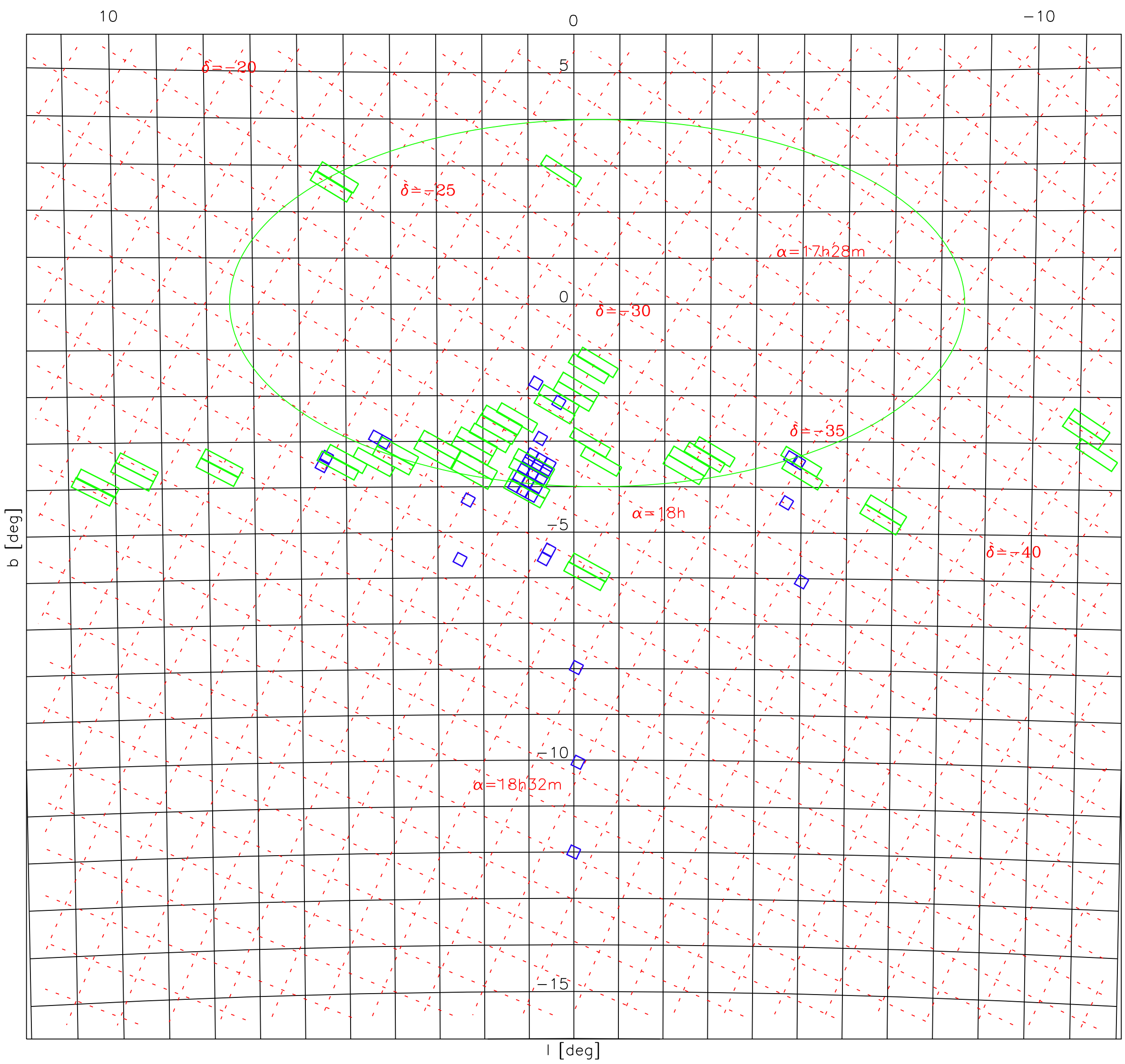

Fig. 1.— OGLE bulge fields in galactic coordinates (gnomonic projection, great circles are mapped to straight lines). Green strips are the OGLE-II scans and blue squares are the old OGLE-I fields. Large oval indicates the location of the Galactic bar. Fields are selected in windows of low extinction and avoid very bright foreground stars.

REFERENCES

Afonso, C. et al. (The EROS Collaboration), 1999, A&A, submitted, astro-ph/9907355

Alard, C., & Lupton, R. H., 1998, ApJ 503, 325

Alard, C., 2000, A&AS, 144, 363

Alcock, C., et al. (The MACHO Collaboration), 1997a, ApJ, 479, 119

Alcock, C., et al. (The MACHO Collaboration), 1997b, ApJ, 482, 89

Alcock, C., et al. (The MACHO Collaboration), 1997c, ApJ, 486, 697

Allsman, R. A., & Axelrod, T. S., 2001, astro-ph/0108444

Brunner, R. J., Djorgovski, S. G., Prince, T. A., & Szalay, A. S., 2001, Invited Review for the Handbook of Massive Datasets, eds. J. Abello, P. Pardalos, and M. Resende, astro-ph/0106481

Mizerski, T., & Bejger, M., 2001, astro-ph/0110375

Sackett, P. D., 1999, Invited Targeted Talk at "Gravitational Lensing: Recent Progress and Future Goals," 28 July 1999, Boston. ASP Conference Series, eds. T.G. Brainerd and C.S. Kochanek., astro-ph/0001048

Szalay, A. S., 2001, in ASP Conf. Serr., Vol. 238, Astronomical Data Analysis Software and Systems X, eds. F. R. Harnden, Jr., F. A. Primini, & H. E. Payne (San Francisco: ASP), 3, astro-ph/0106481

Udalski, A., Kubiak, M., & Szymański, M., 1997, Acta Astron., 47, 319

Udalski, A., Soszyński, I., Szymański, M., Kubiak, M., Pietrzyński, G., Woźniak, P. R., & Żebruń, K., 1998a, Acta Astron., 48, 563

Udalski, A., Szymański, M., Kubiak, M., Pietrzyński, G., Woźniak, P. R., & Żebruń, K., 1998b, Acta Astron., 48, 147

Udalski, A., Soszyński, I., Szymański, M., Kubiak, M., Pietrzyński, G., Woźniak, P. R., & Żebruń, K., 1999a, Acta Astron., 49, 223

Udalski, A., Soszyński, I., Szymański, M., Kubiak, M., Pietrzyński, G., Woźniak, P. R., & Żebruń, K., 1999b, Acta Astron., 49, 437

Udalski, A., Szymański, M., Kubiak, M., Pietrzyński, G., Soszyński, I., Woźniak, P. R., & Żebruń, K., 2000a, Acta Astron., 50, 307

Udalski, A., Żebruń, K., Szymański, M., Kubiak, M., Pietrzyński, G., Soszyński, I., & Woźniak, P. R., 2000b, Acta Astron., 50, 1

Woźniak, P. R., 2000, Acta Astron., 50, 421

Woźniak, P. R., Udalski, A., Szymański, M., Kubiak, M., Pietrzyński, G., Soszyński, I., & Żebruń, K., 2001, Acta Astron., 51, 175

Żebruń, K., Soszyński, I., Woźniak, P. R., Udalski, A., Kubiak, M., Szymański, M., Pietrzyński, G., Szewczyk, O., & Wyrzykowski, Ł, 2001, astro-ph/0110623

6. APPENDIX A

Catalog flags are coded as single bits of a 4 byte integer and listed below (the least significant bit first). Integer value 12, e.g., means that flags 3 and 4 are true and the rest are false. The values quoted for selected pipeline parameters have been actually used to set the flags in this analysis.

1. crowding flag, set if within ± 4 pixels of the maximum pixel with flux f_0 there is a secondary local maximum with pixel flux $f > 0.15 \times f_0 \times r$, where r is the distance from the star centroid in pixels
2. fewer than `N_FRAMES` $=$ `4` used in centroid finding
3. more than `N_BAD` $=$ `0` bad pixels on the reference image within the fitting radius of 3.0 pixels
4. fraction of less than `MIN_GFRA` $=$ `0.5` difference flux measurements are "good" from the total number of frames taken for the field. A "good" point is the one for which non of the several types of problems monitored by the pipeline occurred (flags 1–10 in Appendix B are set to 0).
5. mean magnitude and its scatter could not be calculated because fewer than 2 individual magnitudes were defined

7. APPENDIX B

Light curve flags are coded as single bits of a 4 byte integer and listed below (the least significant bit first). Integer value 12, e.g., means that flags 3 and 4 are true and the rest are false. The values quoted for selected pipeline parameters have been actually used to set the flags in this analysis.

1. pipeline returned error code for difference flux
2. pipeline returned error code for flux error
3. χ^2 per pixel of the difference subframe larger than `MAXCHI2I` = `6.0`
4. χ^2 per pixel of the PSF fit larger than `MAXCHI2N` = `1.0e32` (effectively no cut)
5. FWHM of the PSF fit larger than `MAX_FWHM` = `3.4` pix
6. number of bad pixels within the fitting radius larger than `MAX_NBAD` = `3`
7. correlation coefficient with the PSF lower than `MIN_CORR` = `0.0` (effectively no cut)
8. star in the rejected region of the CCD (currently empty)
9. flux error `NSIGERR` = `10` times larger than percentile `ERRFRAC` = `0.5` of all individual flux errors (0.5 corresponds to median)
10. χ^2 per pixel of the PSF fit `NSIGCHI2` = `10` times larger than percentile `CHI2FRAC` = `0.5` of all individual values (0.5 corresponds to median)
11. magnitude could not be calculated due to missing or non positive fluxes
12. magnitude error could not be calculated due to missing or non-positive values

8. APPENDIX C

Explanation of light curve cleaning parameters. The values quoted have been used to set the flags in Appendices A and B.

1. [`MAXNMAD0` = `0`] — max number of bad pixels on the reference image within the fitting radius
2. [`MINNFRM0` = `4`] — min number of frames used in centroid calculation
3. [`MAX_NBAD` = `3`] — max number of bad pixels on a given image within the fitting radius
4. [`MIN_GFRA` = `0.5`] — min fraction of good points within entire sequence of frames
5. [`BAD_FLUX` = −`99.0`] — error code for difference flux
6. [`BAD_ERR` = −`99.0`] — error code for flux error
7. [`MAXCHI2N` = `1.0e32`] — max χ^2 per pixel for PSF fit
8. [`MAXCHI2I` = `6.0`] — max χ^2 per pixel for difference subframe
9. [`MIN_CORR` = `0.0`] — min correlation coefficient with the PSF
10. [`MAX_FWHM` = `3.4`] — max FWHM in pixels
11. [`ERRCLN` = `1`] — is flagging of large error bars on ? (1 = yes)
12. [`NSIGERR` = `10.0`] — base threshold is multiplied by this factor to get the final threshold for error bar
13. [`ERRFRAC` = `0.5`] — percentile of the error distribution for base threshold
14. [`CHI2CLN` = `1`] — is flagging poor PSF fits on ? (1 = yes)
15. [`NSIGCHI2` = `10.0`] — base threshold is multiplied by this factor to get the final threshold for χ^2 of the PSF fit
16. [`CHI2FRAC` = `0.5`] — percentile of the χ^2 per pix distribution for base threshold